ISSN 1 746-7233, England, UK
World Journal of Modelling and Simulation
Vol. 13 (2017) No. 1, pp. 45-51

Modelling of pulse thermography for defect detection in aluminium structures: Assessment on reflection and transmission measurement*

Ranjit Shrestha[1] , Wontae Kim[2†]

Department of Mechanical & Automotive Engineering, Kongju National Univeristy ,1223-24, Cheonan-daero, Sebuk-gu, Cheonan-si, Chungcheongnam-do, 31080, South Korea

(*Received May 18 2016, Accepted November 14 2016*)

Abstract. This paper presents the study of pulse thermography with reflection and transmission measurement using commercial finite element modelling computer package ANSYS Version 15.0'. A finite element analysis is applied to the 3-Dimensional solid body made of aluminium with known thermal properties and subsurface defects of different size and depth to simulate the heat flow in the pulse thermography inspection process. With the intention to reap the information about defects, the material response to the thermal stimulus is studied. The results show that reflection measurement is suitable for analysing close to surface defects located at the thermal stimulator side and the transmission measurement is more appropriate for analysing deeper defects some distance from the thermal stimulator side.

Keywords: aluminium structures, finite element analysis, infrared thermography, pulse thermography, reflection measurement, transmission measurement

1 Introduction

The natural qualities of aluminium and its alloys are positive deciding factors for designers, manufacturers and industrial users who are consistently on the lookout for better-performing materials and innovative processes. Aluminium, at present is the leading non-ferrous metal in use, finding ever more ingenious applications in sectors as diverse as aeronautics, beverage containers, construction and energy transportation[2]. High quality of materials and structures is an important factor in many areas of human activities. A major effort to reach the highest level of quality is to implement various inspection tasks. Non-destructive testing and evaluation (NDT&E) technique is one of the most important means to detect and verify the quality of items[10, 13, 16].

Infrared thermography (IRT) is an emerging NDT&E technique that enables the non-contact inspection and monitoring of systems and materials through mapping thermal patterns on the surface of the object of interest. IRT requires the creation of the temperature gradient between the defect and non-defect regions to permit defect detection. If a temperature gradient between the scene and the object of interest exist, the target can be inspected using the passive approach. However, when the object or feature of interest is in equilibrium with the rest of the scene, it is possible to create a thermal contrast on the surface using a thermal source which is known as the active approach. In the active approach, pulsed thermography (PT), lock-in hermography (LIT) and vibrothermogragy (VT) are the most commonly used approaches[1, 3, 4, 7, 11, 14, 15, 18, 20].

Finite Element Analysis (FEA) is used to foretell the experimental outcome with certain conditions on account that the experiments are difficult to implement and are expensive. FEA is extensively adopted by many

* This work was supported by the National Research Foundation of Korea (NRF) grant funded by the Korea government (MEST) (NRF-2014R1A1A2054595).

† Corresponding author. *E-mail address*: kwt@kongju.ac.kr.

industries and researchers for modelling and simulation on account that it's faster and cheaper than physical testing[9, 13].

This study focuses on the modelling and simulation of IRT for the detection of defects in aluminium structures. The PT is taken into consideration to obtain the physical insight of the thermal phenomena occurring during and after thermal excitation of the structures. A qualitative comparison of PT with reflection measurement and transmission measurement is presented in this paper.

2 Pulsed thermography

In PT, the specimen surface is submitted to a short heating pulse utilizing a high power optical source. The duration of the pulse may vary from a few milliseconds (2-15 ms utilizing flashes) to several seconds (utilizing lamps). This heating produces a thermal pulse that propagates into the sample by means of thermal diffusion. In the course of the pulse propagation, an infrared camera is used to record the temperature distribution on the sample surface. A subsurface defect, if present, modifies the diffusion heat flow, so its location appears as an area with a temperature difference with respect to the neighborhood region[6, 17]. There are two common modes in PT: reflection and transmission. In reflection mode, the heat source and IR camera are placed at the same side and the reflected thermal wave effect on the surface temperature is continuously monitored. In the transmission mode, the IR camera is placed opposite side to the heat source. The Fig. 1 shows the basic principle of reflection and transmission modes of measurement [19, 21].

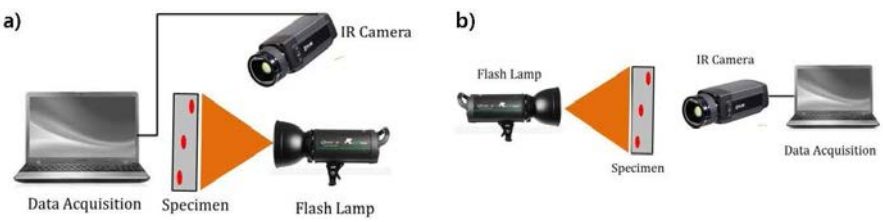

Fig. 1: Schematic of pulse thermography, a) Reflection measurement and b) Transmission measurement

The temperature rise caused by pulse heating of the surface of a semi-infinite sample can be expressed as [8, 12],

$$T = \frac{Q}{2\sqrt{\pi\kappa\rho C t}}, \tag{1}$$

where $T[^{\circ}\mathrm{C}]$ is the temperature rise at time t after the flash heating,Q [W/m^2] is the energy deposited on the surface, k [W/m$^{\circ}$C] is the thermal conductivity, ρ [kg/m^3] is the density of the material and C [J/kg$^{\circ}$C] is the specific heat capacity of the sample material.

The characterization of the defect in any PT measurement is based on the temperature difference created with the aid of defect on the sample surface which is often called thermal contrast. The thermal contrast is the thermal difference in the region to be analysed with recognised reference area which is believed to be pre-chosen. The reference area is considered to be the pure area where no subsurface defect is present. In most cases the reference area is a background in the thermal image. The absolute contrast is defined as the excess temperature over a defect-free region at a given time t and is given by [5, 6],

$$C_{\mathrm{abs}}(t) = T_{\mathrm{defect}}(t) - T\mathrm{sound}(t), \tag{2}$$

where T_{defect} is the temperature over a defect region and T_{sound} a defect-free region, respectively.

3 Model configuration

To simulate the PT inspection, 3D heat flow simulation model has been developed by using a commercial finite element modelling computer package 'ANSYS Version 15.0'. A square shaped (180 mm * 180 mm) aluminium specimen with 10 mm thickness and artificial defects with circular cutouts of varying depth and diameter at back side was considered. Fig. 2(a) shows the geometrical details of the test sample. The idealized shape of a circular defect was chosen to illustrate the effect of geometry on the observed thermal response. Fig. 2(b) shows the front side and Fig. 2(c) shows the rear side of FEA model. Fig. 2(d) shows the FEA model of the specimen with meshing. During meshing, a tetrahedral meshing was adapted. Physical preference was taken as mechanical with relevance 100, relative center was kept in fine mode, proximity and curvature was kept on in advanced size function in order to calculate temperature variations with sufficient spatial resolution.

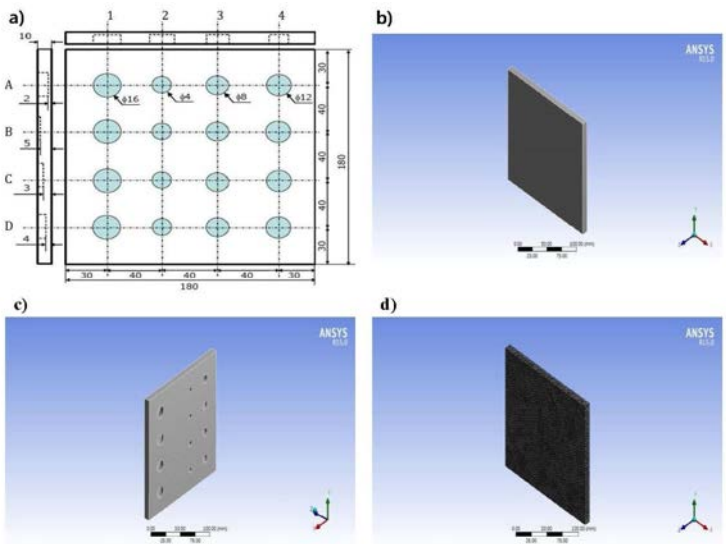

Fig. 2: Model configuration, a) Geometrical details of the test sample, b) Front side of FEA model, c) Rear side of FEA model and d) FEA model with meshing

Table 1: Geometrical parameters & properties

Parameters	Value	Unit
Length (X)	180	mm
Length (Y)	180	mm
Length (Z)	10	mm
Mass (m)	0.87033	kg
Volume (v)	3.14E+05	mm^3
Thermal Conductivity (k)	1.51E-02	W/mm/°C
Specific Heat (C)	480	J/kg/°C
Density (ρ)	2.77E-6	kg/mm^3
Initial Temperature	20	°C
Nodes	80,116	No.
Elements	50,842	No.

The considered thermal properties and geometrical parameters of the specimen are shown in the Table 1. The sample was vertically placed in the surrounding of known temperature. The front surface was stimulated at the beginning of the simulation with calculated pulse heat flux over a 10 ms time interval. It is assumed that the stimulation is uniform and the influence of radiative and convective heat transfer is neglected. The boundary condition for the heat flux is given by Eq. (3),

$$(k.\nabla T) = \phi_0, \tag{3}$$

where, ϕ_0 is the term which describes the heat flux on the irradiated surface.

The ambient temperature Tamb measured in the room was used both as boundary condition and initial condition since it was assumed that the specimen was in equilibrium with the environment at room temperature before the experiment started,

$$T(x, y, z, t) = T_{\text{amb}} = 20^{\circ}. \tag{4}$$

4 Results and discussions

The response to the applied heat flux with each reflection mode and transmission mode was simulated using the transient analysis mode over a period of 6 second. Fig. 3 shows the maximum and minimum surface temperature decay in reflection and transmission mode with respect to time. Due to the very short heat impulse time the temperature rise is faster than its decay. As the time passes, due to thermal diffusion in all directions, the temperature on the sample surface trends towards the equilibrium again. As shown in Fig. 3, it is observed that the cooling process of the specimen is almost over in 3 second in reflection mode and goes up to 5 second in transmission mode. It is also observed that the surface temperature of the specimen is recorded higher in transmission mode in comparison to reflection mode.

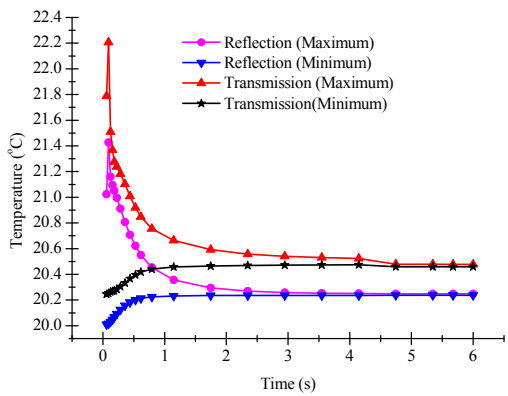

Fig. 3: Surface temperature decay profile

Fig. 4 shows the thermal images recorded at time 0.1 s, 0.3 s and 0.5 s with reflection and transmission mode. In both cases, it is observed that the shallower defects are clearly visible and easily detachable whereas the deeper defects are much faded. The results also show that the shallow defects appear at first and the deepest defects become visible later in both cases. However, only some of the deep defects are visible in reflection measurement in comparison to transmission measurement. The unique feature that helps precisely to recognize a defect is the difference of temperature between the defect and defect-free areas. The temperature above the defect is higher than in the neighborhood. The noticeable temperature difference indicates the presence of a defect and pinpoints its location.

Absolute contrast method was used to compute the temperature difference between the defect region and the defect-free region for the defect characterization purpose. The absolute contrast was evaluated by subtracting the temperature value located centrally over the defects from the temperature value measured in defect-free region near the defects. Analysis of thermal image is done in relation to both defect depth and defect size with respect to time.

To inquire into the effect of defect depth on absolute contrast; defects,$A_1, C_1, D_1 \& B_1$ with depth 2,3,&5 mm respectively and the fixed diameter 16 mm were selected. The absolute contrast measured over the defects as a function of defect depth fortime of 6 second is shown in the Fig. 5. As can be seen in Fig. 5, the absolute contrast decreases with the increasing defect's depth for the fixed defect size.

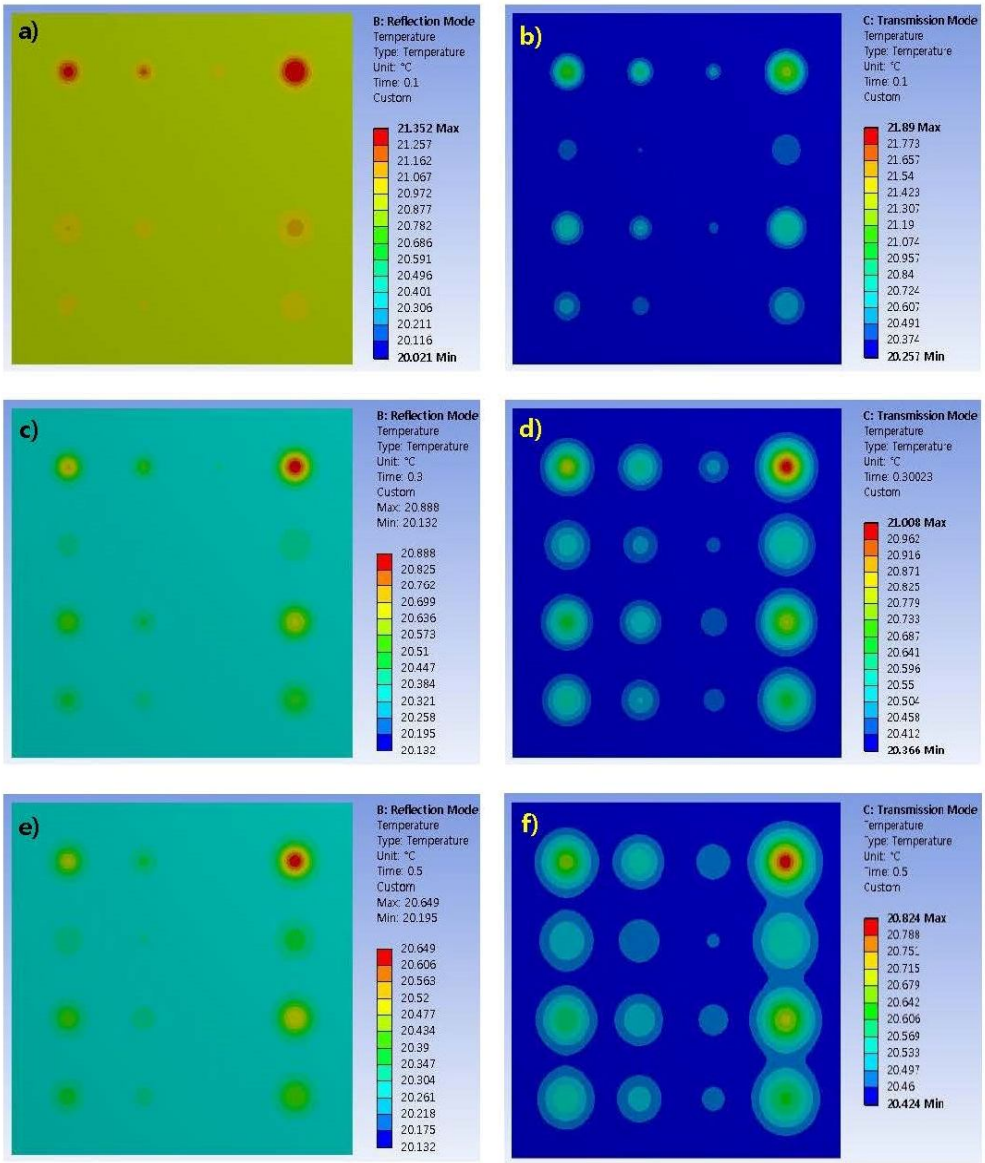

Fig. 4: Thermal images at different time interval, a) Thermal image at time 0.1 s with reflection measurement, b) Thermal image at time 0.1 s with transmission measurement, c) Thermal image at time 0.3 s with reflection measurement, d) Thermal image at time 0.3 s with transmission measurement, e) Thermal image at time 0.5 s with reflection measurement and f) Thermal image at time 0.5 s with transmission measurement.

To inquire into the effect of defect size on absolute contrast; defects, $A_2, A_3, A_4, \& A_1$with diameter 4, 8, 12& 16 mm respectively and fixed depth 8 mm were considered. The absolute contrast measured over the defects as a function of defect size for a time of 6 seconds is shown in Fig. 6. As can be seen in Fig. 6, the absolute contrast increases with the increasing defect's size for the fixed defect depth. From Fig. 5 and Fig. 6, it is confirmed that the absolute contrast is a function of defect size and depth.

5 Conclusion

Detection of defects by modelling of pulsed thermography has been found to be an important research topic in the last years. A finite element modelling scheme using 'ANSYS Version 15' is proposed to completely simulate the pulse thermography for the detection of defects in aluminium structures. The result shows that the temperature distribution on the specimen surfaces depends on material properties, boundary conditions, heat stimulation intensity, and duration. It was found that reflection measurement enables a high resolution for the

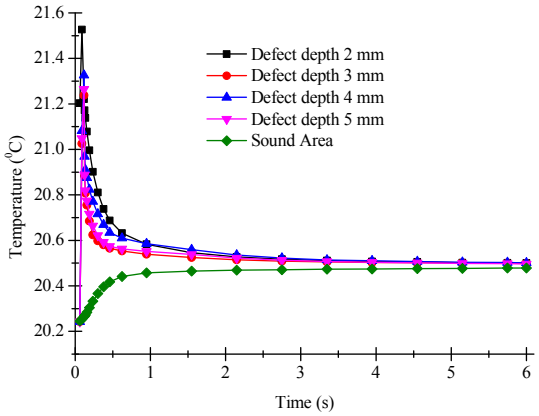

Fig. 5: Absolute contrast vs. defect depth for defect size 16 mm

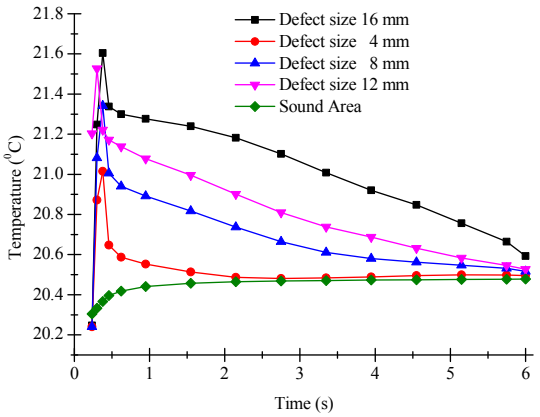

Fig. 6: Absolute contrast vs. defect size for defect depth 2 mm

detection of defects, but it could only detect the defects close to the heating surface. For detecting deep defects, transmission measurement was found appropriate at the peak temperature time. It is also found that high heat flow value gives a greater temperature difference in the defect's surface and is favourable for the defect detection. The absolute contrast depends on the variation of the defect depth and size; ie it decreases with the increase in defect depth andincreases with the increases in defect size. It is concluded that this technique is capable of detecting and reconstructing subsurface defects in 3D. With the assumption of transient heat flow condition and concerning the thermal response of defective region, the FEA gave the correct predictions for the thermal images and the size of defect.

References

[1] C. I. Castanedo. Quantitative subsurface defect evaluation by pulsed phase thermography: depth retrieval with the phase [ressource lectronique] /. 2005.

[2] C. T. Center. *Aluminium properties and applications*. Constellium C-TEC brochure., 2015.

[3] Y. Duan, S. Huebner, et al. Quantitative evaluation of optical lock-in and pulsed thermography for aluminum foam material. *Infrared Physics & Technology*, 2013, **60**(5): 275–280.

[4] C. Ibarra-Castanedo, J.-M. Piau, et al. Comparative study of active thermography techniques for the nondestructive evaluation of honeycomb structures. *Research in Nondestructive Evaluation*, 2009, **20**(1): 1–31.

[5] C. A. Larsen. Document flash thermography. *Dissertations & Theses - Gradworks*, 2011.

[6] S. Lugin. Algorithms for efficient and quantitative non-destructive testing by pulsed thermography. *Defect Detection*, 2007.

[7] C. Meola, G. M. Carlomagno. Recent advances in the use of infrared thermography. *Measurement Science & Technology*, 2004, **15**(9): R27–R58(32).

[8] S. Pickering, D. Almond. Matched excitation energy comparison of the pulse and lock-in thermography nde techniques. *Ndt & E International*, 2009, **41**(7): 501–509.

[9] S. Ranjit. Numerical simulation for quantitative characterization of defects in metal by using infra-red thermography. *International Journal of Applied Engineering Research*, 2014, **9**(24): 29939–29948.

[10] S. Ranjit. Research on defects detection by image processing of thermographic images. *International Journal of Engineering & Technology*, 2015, **7**(5): 1849–1855.

[11] S. Ranjit, M. Choi, W. Kim. Quantification of defects depth in glass fiber reinforced plastic plate by infrared lock-in thermography. *Journal of Mechanical Science and Technology*, 2016, **30**(3): 1111–1118.

[12] S. Ranjit, Y. Chung, W. Kim. Thermal behavior variations in coating thickness using pulse phase thermography. *Thermal Behavior Variations in Coating Thickness Using Pulse Phase Thermography*, 2016, **36**.

[13] S. Ranjit, K. Kang, W. Kim. Investigation of lock-in infrared thermography for evaluation of subsurface defects size and depth. *International Journal of Precision Engineering and Manufacturing*, 2015, **16**(11): 2255–2264.

[14] S. Ranjit, W. Kim. Detection and quantification of defects in composite material by using thermal wave method. 2015, **35**(6): 398–406.

[15] S. Ranjit, W. T. Kim. Detection of subsurface defects in metal materials using infrared thermography. *Tropics*, 2014, **19**(2): 1–8.

[16] R. Shrestha, J. Park, W. Kim. Application of thermal wave imaging and phase shifting method for defect detection in stainless steel. *Infrared Physics & Technology*, 2016, **76**: 676–683.

[17] J. G. Sun. Analysis of pulsed thermography method for defect depth prediction. *Journal of Heat Transfer*, 2006, **128**(4): 329–338.

[18] M. Szczepanik, J. Stabik, et al. Detecting of defects in polymeric materials using pulsed infrared thermography. *Archives of Materials Science & Engineering*, 2008, **30**(1).

[19] A. Vageswar, K. Balasubramaniam, C. Krishnamurthy. Wall thinning defect estimation using pulsed ir thermography in transmission mode. *Nondestructive Testing & Evaluation*, 2013, **7**(4): 288–297.

[20] R. C. Waugh. *Development of Infrared Techniques for Practical Defect Identification in Bonded Joints*. Ph.D. Thesis, University of Southampton, 2014.

[21] O. Wysockafotek, M. Maj, W. Oliferuk. Use of pulsed ir thermography for determination of size and depth of subsurface defect taking into account the shape of its cross-section area. *Archives of Metallurgy and Materials*, 2016, **60**(2): 615–620.